Review in Advance first posted online on October 13, 2008. (Minor changes may still occur before final publication online and in print.)

Photoelectron Spectroscopy of Multiply Charged Anions

Xue-Bin Wang and Lai-Sheng Wang

Department of Physics, Washington State University, Richland, Washington 99354, and Chemical and Materials Sciences Division, Pacific Northwest National Laboratory, Richland, Washington 99352; email: ls.wang@pnl.gov

Annu. Rev. Phys. Chem. 2009. 60:105–26

The *Annual Review of Physical Chemistry* is online at physchem.annualreviews.org

This article's doi: 10.1146/annurev.physchem.59.032607.093724

0066-426X/09/0505-0105$20.00

Key Words

intramolecular Coulomb repulsion, repulsive Coulomb barrier, negative electron binding energy, ion solvation, electronic structure, electrospray ionization, low-temperature ion trap

Abstract

Multiply charged anions (MCAs) are common in condensed phases but are challenging to study in the gas phase. An experimental technique, coupling photoelectron spectroscopy (PES) with electrospray ionization (ESI), has been developed to investigate the properties of free MCAs in the gas phase. This article reviews the principles of this technique and some initial findings about the intrinsic properties of MCAs. Examples include the observation of the repulsive Coulomb barrier that exists universally in MCAs and its effects on the dynamic stability and PES of MCAs. The solvation and solvent stabilization of MCAs have been studied in the gas phase and are also discussed. A second-generation low-temperature ESI-PES apparatus has been developed, which allows ion temperatures to be controlled from 10 to 350 K. New results from this low-temperature ESI-PES instrument are also reviewed, including doubly charged fullerene anions, inorganic metal complexes, and temperature-induced conformation changes of complex anions.

1. INTRODUCTION

MCA: multiply charged anion

RCB: repulsive Coulomb barrier

ESI: electrospray ionization

Multiply charged anions (MCAs) are ubiquitous in nature and are important constituents in solutions and solids. Their existence has been generally taken for granted in the teaching of chemistry and in our understanding of materials. However, MCAs are usually rather fragile as isolated species in the gas phase owing to the strong intramolecular Coulomb repulsion among the excess charges and the missing stabilization through solvation and other electrostatic interactions, making many common textbook MCAs unstable and difficult to study (1–4). Despite a handful of mass spectrometric observations of large organic molecular MCAs (5–8), our knowledge about their properties had been limited previously. In 1990, Compton and colleagues' (9) observation of small carbon cluster dianions, C_n^{2-} ($n = 7$–28), stimulated much experimental and theoretical interest in gaseous MCAs.

Early theoretical considerations of MCAs derived from interest in searching for molecular species with unusually high electron affinities (10, 11) and in understanding the electronic structure of condensed-phase species (12, 13). The groups of Cederbaum and Simons have made major theoretical advances in our understanding of MCAs. Cederbaum and coworkers investigated a series of gaseous MCAs (14–29) and proposed a construction principle for predicting gaseous MCAs based on the alkali and alkali-earth halide systems (17, 18). Simons and coworkers (4, 30–36) considered many MCAs that exist in the condensed phase and investigated their structure, bonding, and stability in the gas phase. They proposed concepts of mixed valence–dipole bound and dipole-dipole bound dianions as well (35, 36). There have also been a number of other theoretical studies on gaseous MCAs (37–45), in particular concerning small carbon clusters (15, 19, 37–40) and those relevant to condensed-phase materials (44, 45). The electron-electron repulsion and the resultant repulsive Coulomb barrier (RCB), which originates from the combination of short-range binding and long-range Coulomb repulsion, have been pointed out in several early theoretical works on multiply charged metal clusters, fullerene anions (46–48), and later theoretical models on several small MCAs (24, 25, 49, 50).

Early experimental efforts on gaseous MCAs were all made via mass spectrometric observations using a variety of ionization techniques. These include the observation of doubly charged anions of small carbon clusters (9, 51–53), fullerenes (54–58), and other species (59–62) using the ion-sputtering technique; doubly charged small organic, inorganic, and fullerene anions using electrospray ionization (ESI) (63–72); and multiply charged metal clusters and fullerene anions via sequential electron attachment in a Penning trap (73–76). Recently, several new experimental findings have been reported, including the observation of the short-lived LiF_3^{2-} species (77), a series of new composite small dianions using a sputtering source along with gas flooding (78), and the generation of doubly charged anions via a charge-transfer technique (79–83). The coordination numbers of ligand and solvent molecules required to make stable dianionic metal complexes (84–86) and hydrated clusters (63, 87) have been pursued using size-selected collision-induced dissociation techniques. The competition between ionic fragmentation versus electron detachment and the counter-ion perturbation of MCAs has been investigated by collision excitation and ab initio calculations (88–91). Lifetimes for a number of metastable dianions have been directly measured (83, 92).

Beyond the above mass spectrometric investigations, spectroscopic studies of MCAs remained a challenge. Although a number of doubly charged anions were observed using ion sputtering, laser ablation, and other collisional techniques (9, 51–61), their intensities were too weak to allow for spectroscopic investigations. Conversely, the ESI technique, pioneered by Fenn and coworkers (93, 94) as a soft-ionization method for biomolecules, could produce small gaseous MCAs directly from solutions (63–72), making it a promising technique for spectroscopic studies of these exotic species.

In 1998, we developed an experimental technique combining ESI and photoelectron spectroscopy (PES) to investigate MCAs (95–97). PES is an ideal technique to probe the intrinsic properties of MCAs in the gas phase. It provides direct measurements of the excess electron binding energies in MCAs, thus allowing one to obtain information about their stability and intramolecular Coulomb repulsion. Using this technique, systematic studies have been carried out on a variety of free MCAs, including inorganic and organic MCAs, redox species, and biologically relevant molecules (95–120). Since these initial studies, several other spectroscopic techniques based on ESI have been developed, including photodissociation (121), photodetachment (122–125), and pump-probe experiments (126). Recently we have developed a second-generation ESI-PES apparatus that can selectively trap ions under low-temperature conditions (127–129). Temperature is a critical issue in gas-phase spectroscopy and ion chemistry. The low-temperature trap is valuable to suppress thermal broadening in photoelectron spectra and to help stabilize weakly bound clusters. In addition, temperature-dependent studies are possible, which can be used to investigate entropic effects on ion conformations and isomer populations.

PES: photoelectron spectroscopy

TOF: time of flight

Several reviews and feature articles about gaseous MCAs are now available in the literature (1, 26, 91, 104, 109, 120) with emphasis on early theoretical and experimental advances, including spectroscopic investigations of MCAs at room temperature. In this review, we first give a brief summary of some of the early findings of free MCAs, such as the direct observation of the RCB (96, 97), the experimental observation of negative electron binding energies (102, 103), and the solvation and solvent stabilization of complex MCAs (106–111). Then we focus on progress made using the low-temperature ESI-PES technique. One can effectively cool anions and completely eliminate hot band transitions in PES (127). More accurate electron binding energies and detailed electronic structure information are thus obtained from cold spectra for a number of transition-metal complexes and fullerene dianions (130–134). Temperature-dependent studies on several complex systems display drastic spectral changes as a function of temperature owing to entropy-driven conformation changes, which allows energetic as well as thermodynamic information to be obtained (128, 135).

2. ROOM- AND LOW-TEMPERATURE ELECTROSPRAY ION-TRAP PHOTOELECTRON SPECTROSCOPY

The design and operation of a room-temperature ESI-PES apparatus have been described in detail elsewhere (95). A schematic view of the instrument is given in **Figure 1**, and important features are described below. Solutions containing the anions of interest (typically ~1–0.1 mM in CH_3CN or 3:1 CH_3OH:H_2O) are sprayed through a syringe (~0.04 mL h^{-1}), which is biased at a negative high voltage. Highly charged negative droplets from the syringe are fed into a desolvation capillary maintained at ~50–100°C for desolvation. Anions that emerge from the heated capillary are guided by a radiofrequency-only quadrupole ion guide into a quadrupole ion trap, where ions are accumulated for 0.1 s before being ejected into a time-of-flight (TOF) mass spectrometer. The desired anions are mass selected by a mass gate and decelerated before being detached by a laser beam in the interaction zone of a magnetic-bottle photoelectron analyzer. The photoelectron energies are calibrated with the known spectra of I^-, O^-, or ClO_2^- (136).

The low-temperature ESI-PES apparatus has been described previously (127–129). A key feature of the new apparatus is a temperature-controlled ion trap that is used for ion accumulation and cooling (129). The ion trap is attached to the cold head of a closed-cycle helium refrigerator, which can reach a low temperature of 5 K and can be controlled up to 350 K. The ESI source, TOF mass spectrometer, and magnetic-bottle PES analyzer are similar to the room-temperature instrument described above (95).

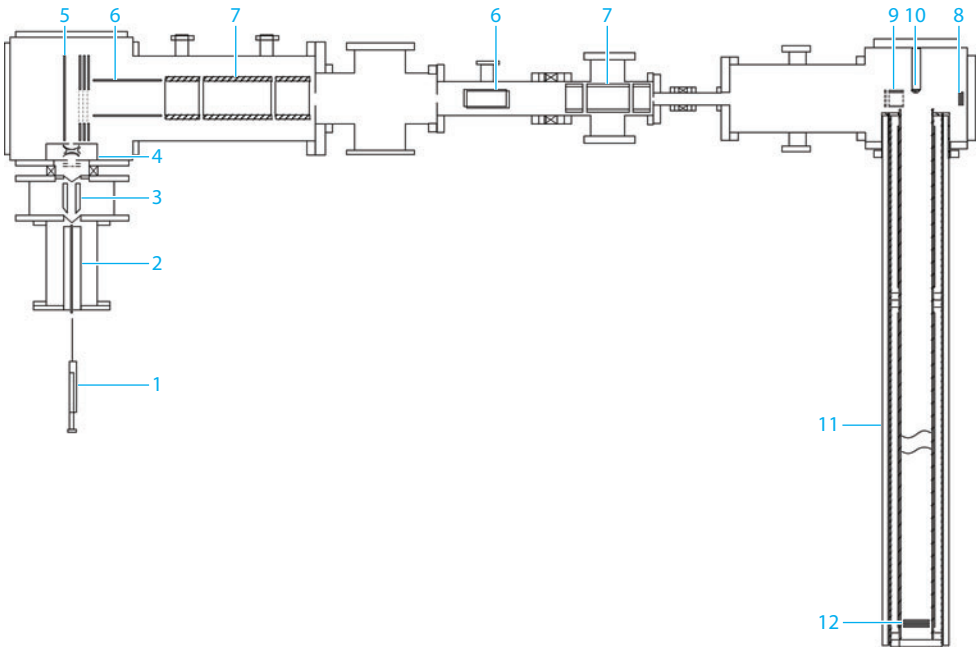

Figure 1

Schematic view of the electrospray photoelectron spectroscopy apparatus: (1) syringe, (2) heated desolvation capillary, (3) radiofrequency quadrupole ion guide, (4) quadrupole ion trap, (5) time-of-flight (TOF) mass spectrometer extraction stack, (6) vertical and horizontal deflectors, (7) Einzel lens assembly, (8) 40-mm dual microchannel plate in-line ion detector, (9) three-grid mass-gate and momentum decelerator assembly, (10) permanent magnet (NdFeB), (11) 4-m TOF tube with a low-field solenoid and double-layer μ-metal shielding, and (12) 40-mm Z-stack microchannel plate photoelectron detector. Figure reprinted from Reference 95.

3. UNIQUE PROPERTIES OF FREE MULTIPLY CHARGED ANIONS

3.1. Direct Observation of the Repulsive Coulomb Barrier, Intramolecular Electron-Electron Repulsion, and Electron Tunneling Through the Repulsive Coulomb Barrier

The universal existence of the RCB, which originates from the combination of the short-range electron binding and long-range Coulomb repulsion between the outgoing detached photoelectron and the remaining anion, was directly observed in the first PES experiment on MCAs: the citrate dianion (CA^{2-}) (**Figure 2**) (96). The 266-nm spectrum (**Figure 2*d***) shows a very broad and asymmetric feature, whereas the 355-nm spectrum (**Figure 2*c***) exhibits a relatively narrow and symmetric band. Close examination of the 266-nm spectrum revealed that it actually contains two overlapping bands, the X band observed in the 355-nm spectrum with an adiabatic detachment energy (ADE) of 1.0 eV and another band at a higher binding energy, the A band, with an ADE of 1.6 eV, as seen more clearly in **Figure 2*e***. There was no photoelectron signal observed at 532 nm even though the photon energy was higher than the ADE of the X band. The photon-energy-dependent spectra vividly demonstrated the existence and effects of the RCB (**Figure 2*b***). The 266-nm photon must be above the RCB of both the X and A states, so both states were observable at 266 nm. The 355-nm photon must be below the RCB of the A state, but higher than that of the X state, so only the X state was accessible at 355 nm. The 532-nm photon must then be lower than

ADE: adiabatic detachment energy

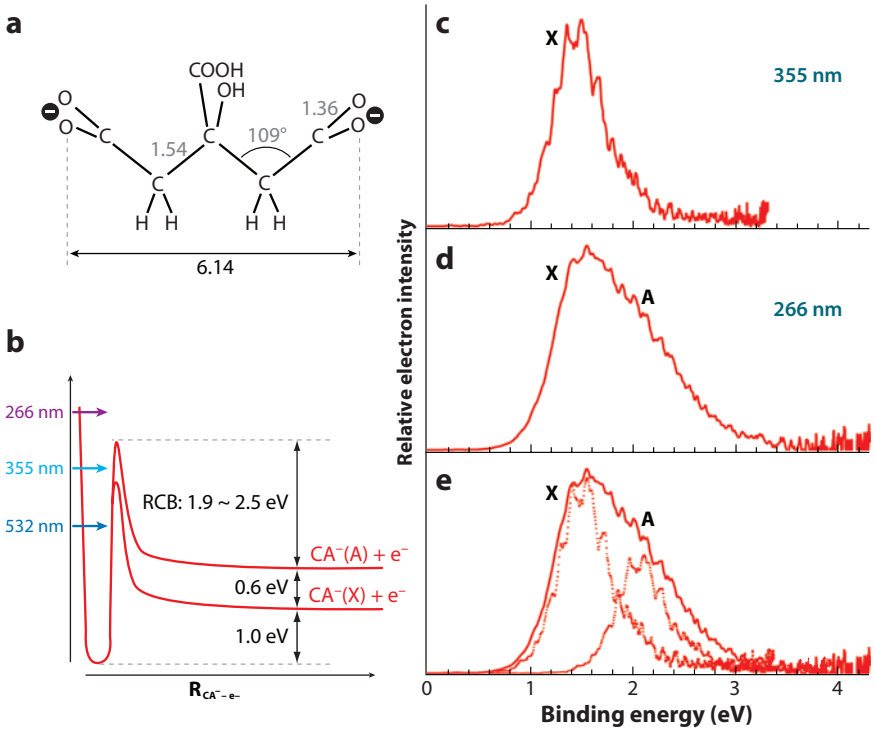

Figure 2

(*a*) Structure of the citrate dianion with relevant bond lengths (Å) and bond angles. (*b*) Schematic potential energy curves showing the adiabatic electron binding energies and the repulsive Coulomb barrier (RCB) for the detachment of CA^{2-}, leading to the X and A asymptotic states of CA^{-}. Note that the barrier heights relative to the X and A states are assumed to be the same. Photoelectron spectra of citrate dianion (CA^{2-}) at (*c*) 355 nm (3.496 eV) and (*d*) 266 nm (4.661 eV). Note the increased spectral width in the 266-nm spectrum, implying an additional detachment channel as shown in panel *e*. Figure reprinted from Reference 96.

the RCB of both the X and A states; thus no signal could be observed at this photon energy. With the assumption that the RCBs of the X and A states are the same, its magnitude can be estimated on the basis of the above photon-energy-dependent information as $1.9 < \text{RCB} < 2.5$ eV. The RCB effectively prevented photoelectrons with kinetic energies less than the height of the RCB from being emitted, resulting in a cutoff in the high binding energy side in the PES spectra. This cutoff has become a hallmark for PES of MCAs.

Subsequently, PES experiments were performed on a series of linear dicarboxylate dianions $^{-}O_2C\text{-}(CH_2)_n\text{-}CO_2^{-}$, where n indicates the aliphatic chain length ($n = 3$–10) (97). These dianions are similar to the citrate dianion, and the two charges are localized on the terminal carboxylate groups, but now the separation between the two charges can be systematically varied. The electron binding energies of these dianions increase linearly with n, whereas the RCB decreases with n. The sum of the two is a constant and close to the electron binding energy of a singly charged carboxylate anion. Therefore, the decrease of the binding energy in the dianions, owing to the presence of the second charge (intramolecular Coulomb repulsion), is equal exactly to the RCB. Thus one can quantitatively determine the amount of intramolecular Coulomb repulsion in MCAs through measurements of the height of the RCB. A similar linear relationship between the proton affinity

and intramolecular Coulomb repulsion is also found computationally in a series of dications, separated by organic spacer groups (137).

Analogous to the α-decay phenomenon, quantum-tunneling effects are expected to occur through the RCB when the detachment photon energies are above the binding energy of an MCA, but below the RCB. Indeed, such tunneling effects have been observed in the short-chain dicarboxylate dianions at 532 nm and have been modeled quantitatively using the WKB formalism (100). The modeled tunneling probabilities decrease rapidly for the larger dianions, consistent with experimental observation.

3.2. Observation of Negative Electron Binding Energy and Electronically Metastable Multiply Charged Anions

In MCAs, the RCB provides dynamic stability, and in principle, it can even trap unbound excess electrons from immediate autodetachment. In other words, it should be possible to observe MCAs with negative electron binding energies. Many familiar textbook MCAs (such as SO_4^{2-}, CO_3^{2-}, and PO_4^{3-}) have negative electron binding energies that are so high they become unstable and have never been observed in the gas phase (1, 4). One obvious target is C_{60}^{2-}, which is predicted theoretically to have a negative electron binding energy as high as −0.3 eV (1, 46) and has been observed in the gas phase (54, 55). However, we were not successful in producing C_{60}^{2-} with our electrospray source. Other groups also failed to observe C_{60}^{2-} using electrospray. The previous sightings of C_{60}^{2-} were both done with laser desorption in an ion-cyclotron resonance mass spectrometer (54, 55) and via charge transfer between C_{60}^{-} and Na (81). The lifetime of an isolated C_{60}^{2-} has been recently measured to be only ∼1 ms using an ion storage ring device (83).

The first successful observation of a negative electron binding energy came as a complete surprise in a quadruply charged anion, 3,4′,4′,4″-tetrasulfonate copper phthalocyanine, $[CuPc(SO_3)_4]^{4-}$ (**Figure 3**) (102). This MCA is produced abundantly by the electrospray of a sodium salt solution. The 193-nm spectrum reveals a weak feature (X) at negative binding energies with the threshold energy of −0.9 eV and two broad features (A and B) at higher binding energies. At 266 nm, the negative–electron binding energy feature becomes dominant, the higher–binding energy feature B disappears, and only a tail of the feature A is observed owing to the RCB. The observation of the negative–binding energy feature is remarkable, indicating that the photoelectron kinetic energy corresponding to this feature is 7.32 eV at 193 nm (i.e., 0.9 eV higher than the photon energy). The PES spectra of $[CuPc(SO_3)_4]^{4-}$ are similar to that of the neutral parent CuPc molecule, except the neutral CuPc has a much higher electron binding energy with a threshold ionization potential of 6.3 eV. The similarity between the PES spectra of the charged species and that of the parent CuPc suggests that detachment occurs from molecular orbitals mainly of CuPc character in the anions. A simple electrostatic estimation indicates that the four negative charges would create a 7.2-eV negative potential on the central Cu atom (i.e., an electron localized on Cu would experience a Coulomb repulsion of 7.2 eV), giving rise to a −0.9-eV (6.3–7.2 eV) binding energy, in excellent agreement with experimental observation. We observed no measurable ion loss within the period of 400 s that we could store the ions. The long lifetime of this metastable tetraanion in the gas phase is also surprising and can be attributed to the large barrier height (estimated to be 3.5 eV) and the large size of the molecule. The RCB can be viewed as an electrostatic corral in this semiplanar molecule, trapping the negatively bound electron inside. Kappes' group (125) confirmed this observation and also measured the lifetime of the metastable anions more accurately. Negative electron binding energies have also been observed in two small dianions, $PtCl_4^{2-}$ and $PtBr_4^{2-}$, with the adiabatic electron binding energies of −0.25 and −0.04 eV, respectively (103), as well as in a large triply charged anion with an −0.66-eV electron binding energy recently (138).

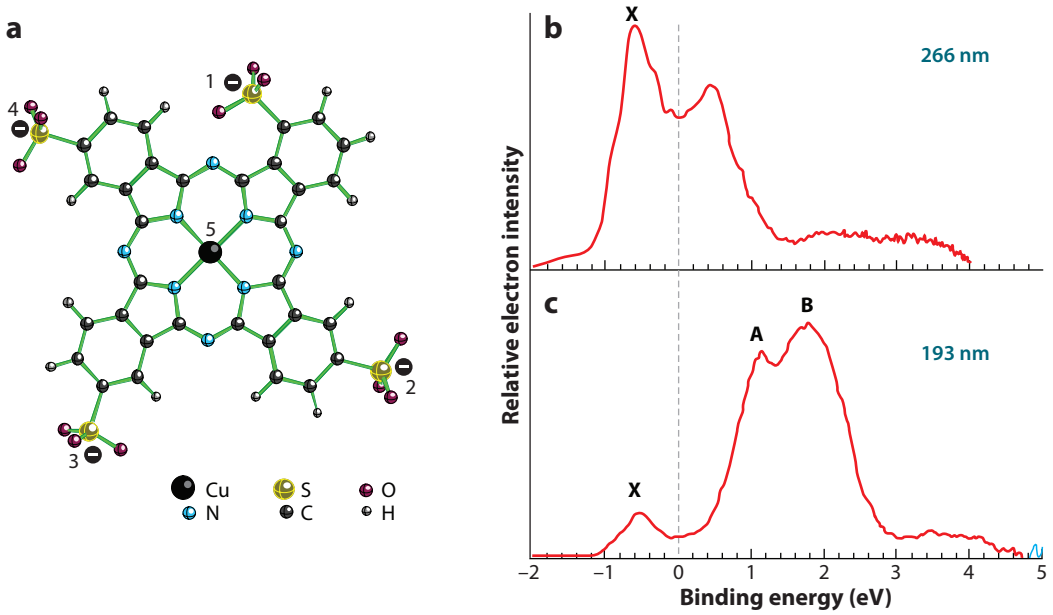

Figure 3

(*a*) Structure of the $[CuPc(SO_3)_4]^{4-}$ tetraanion. Photodetachment spectra of $[CuPc(SO_3)_4]^{4-}$ at (*b*) 266 nm and (*c*) 193 nm. Note the negative–electron binding energy feature (X) of the tetraanion. The dashed line indicates the zero binding energy mark. Figure reprinted from Reference 102.

4. STABILIZATION AND MICROSOLVATION OF COMPLEX MULTIPLY CHARGED ANIONS IN THE GAS PHASE

4.1. Solvation and Solvent Stabilization of Electronically Unstable Multiply Charged Anions: From Gas-Phase Clusters to Bulk Solutions

Many familiar and common inorganic MCAs (such as SO_4^{2-}, CO_3^{2-}, and PO_4^{3-}) are not electronically stable in the gas phase because of the tremendous intramolecular Coulomb repulsions. These anions exist in the condensed phase and are stabilized by solvation in solutions or counter-ions in solids (1, 4, 139). It would be of fundamental chemical and physical significance to understand how MCAs are stabilized in the gas phase by solvents or counter-ions. We have carried out a series of experiments to address the stabilization and solvation of SO_4^{2-} and $C_2O_4^{2-}$ by water in the gas phase (106–108). Three water molecules are the minimum required to stabilize SO_4^{2-} and $C_2O_4^{2-}$ in the gas phase, and the solute dianions are solvated in the center of the water cluster. Photoelectron spectra of small clusters were characteristic of the respective solutes, but beyond the first solvation shell, photoemission features from the solutes were diminished, and a new feature from the ionization of water emerged, analogous to bulk aqueous solutions. A smooth transition from gas-phase clusters to the behavior of electrolyte solutions was clearly revealed, and the large solvated clusters can be used as molecular models to investigate the photophysics and chemistry of aqueous electrolyte solutions. Ab initio calculations for small hydrated sulfate and oxalate clusters showed that the water molecules tend to solvate symmetrically around SO_4^{2-} and $C_2O_4^{2-}$ (106, 108). Subsequent theoretical calculations and molecular dynamic simulations confirm the behavior of the interior solvation of sulfate in the solvated clusters (140–143).

4.2. Solvent-Mediated Folding of Doubly Charged Anions, and Bulk Versus Interfacial Aqueous Solvation

Linear dicarboxylate dianions $^{-}O_2C\text{-}(CH_2)_n\text{-}CO_2^{-}$ have two distinct charged groups ($\text{-}CO_2^{-}$) linked by a flexible aliphatic chain, and the hydrated clusters represent a simple model system to study the hydrophilic and hydrophobic interactions. We investigated the microsolvation of these dianions ($n = 2, 4, 6, 12$) by PES and molecular dynamics simulations one solvent molecule at a time for up to 20 water molecules (110, 111). The two charge centers are solvated separately and alternately. As the solvent number increases, the competition between the Coulomb repulsion and water-water interactions leads to a conformation change, in which the linear dianions become bent so that the two solvation centers merge to enhance the water-water cooperative hydrogen-bonding interactions (**Figure 4**). For the solvated suberate dianion $^{-}O_2C(CH_2)_6CO_2^{-}(H_2O)_m$, the conformation change occurs at $m = 16$. The competition between hydrophilic interactions of the charged carboxylate groups and hydrophobic interactions of the aliphatic chain leads to a transition from bulk aqueous solvation of small dicarboxylates ($n < 4$) to surface solvation for the larger dicarboxylates. These size-dependent solvation behaviors may have implications for heterogeneous chemistry at aqueous surfaces and for atmospheric chemistry.

Molecular dynamics simulations reveal that the cluster temperature also plays an important role in the conformation change owing to the entropic effect (110). For example, simulations indicate that at 150 K the suberate conformation change occurs with 16 water molecules, but at 230 K the conformation change occurs with 23 water molecules. This is because the linear configuration is more flexible and has a larger entropic contribution to its free energy compared to the folded conformation at finite temperatures. As discussed in Section 5, we have carried out a temperature-dependent study on the solvation and conformation change of the suberate dianion using a low-temperature apparatus in the range of 18 to 300 K. Dramatic spectral changes as a function of temperature are observed, allowing quantitative evaluations of the entropic and enthalpic effects on the folding transition.

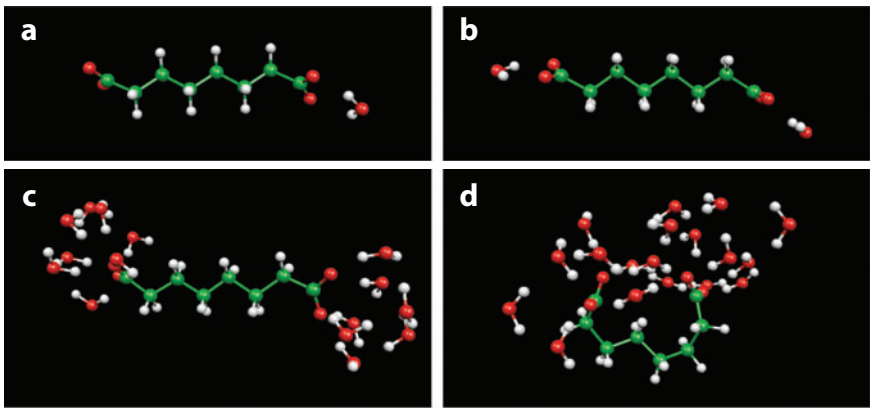

Figure 4

Snapshots from simulations of the suberate dianion with (*a*) one, (*b*) two, (*c*) 15, and (*d*) 18 water molecules (folded structure). Figure reprinted from Reference 110.

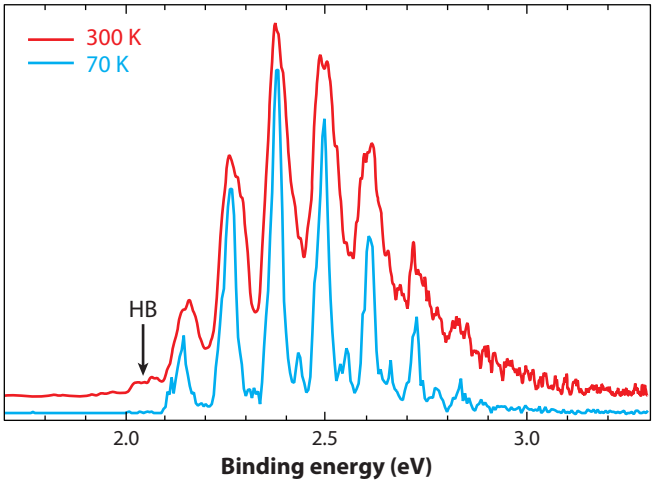

Figure 5

Photoelectron spectrum of ClO_2^- at 355 nm and two temperatures: 300 and 70 K. HB represents hot-band transitions. Figure reprinted from Reference 129.

5. LOW-TEMPERATURE PHOTOELECTRON SPECTROSCOPY OF MULTIPLY CHARGED ANIONS AND TEMPERATURE-DEPENDENT STUDIES

The ability to control ion temperatures is critical for gas-phase spectroscopy and has been a challenge in chemical physics. Recently a second-generation ESI-PES instrument was developed to control anion temperatures for PES studies (127–129). Ion cooling is accomplished in a Paul trap via collisions with a background gas, and ion temperatures can be tuned from 10 to 350 K. Cold anions are demonstrated by the observation of H_2 condensation on trapped ions (129). Vibrational cooling for both simple and complex anions is observed, yielding considerably better resolved photoelectron spectra (127, 133, 134). **Figure 5** shows the 355-nm PES spectrum of ClO_2^- at 70 K compared with that at 300 K. Even at the moderate low temperature of 70 K, the hot band in the PES spectrum is completely eliminated, resulting in a much better resolved spectrum, in which the bending mode (weak peaks between the intense stretching vibrational peaks) is clearly resolved. Even though the spectral resolution is not high in the current magnetic-bottle instrument, the spectral information in the low-temperature data of ClO_2^- is similar to that obtained in a previous high-resolution PES spectrum (136). More importantly, temperature-dependent PES studies are now possible and have been carried out on a number of complex systems, revealing drastic spectral changes due to conformation changes at low temperatures (128, 135).

5.1. Temperature-Dependent Photoelectron Spectroscopy of Hydrated Suberate Dianions: Observation of Entropic Effects

Figure 6 compares the PES spectra of $^-O_2C\text{-}(CH_2)_6\text{-}CO_2^-(H_2O)_n$ ($n = 13$–17) at three trapping temperatures. As discussed above, the room-temperature hydrated clusters show a continuous increase of electron binding energies until $n = 16$, at which the PES spectrum exhibits a sudden shift to a lower electron binding energy, signaling a linear-to-folded transition. Because of entropic effects, it is expected that the number of water molecules required to induce the folding transition should be smaller at lower temperatures. Indeed, at 82 K the PES spectrum of $n = 14$ displays

Figure 6

Comparison of the photoelectron spectra of hydrated suberate $^{-}O_2C\text{-}(CH_2)_6\text{-}CO_2^{-}(H_2O)_n$ (n = 13–17) at 193 nm (6.424 eV) at 82 K (*gold*) and 18 K (*blue*) with those at room temperature (*red*).

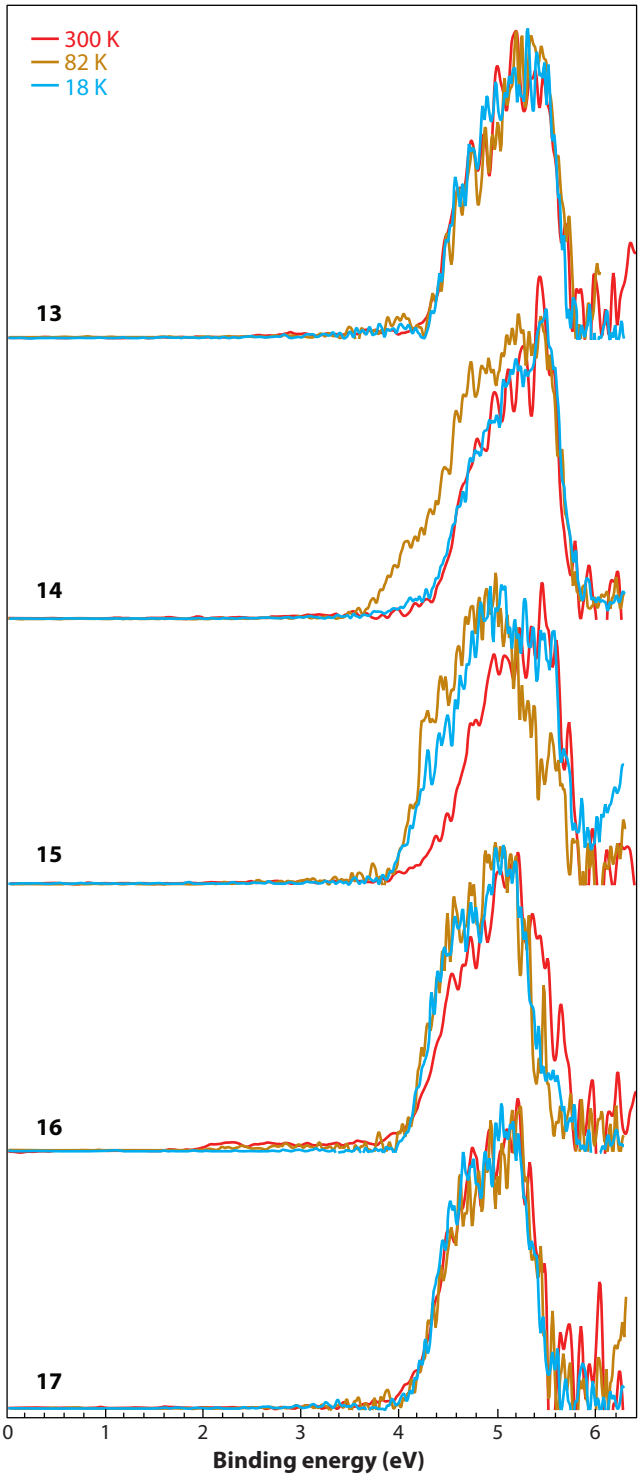

a lower binding energy feature, indicating the onset of folding. The 82-K spectrum of $n = 15$ shows a major shift to lower binding energies, implying a folded conformation at low temperatures. The threshold electron binding energy of $n = 14$ at 82 K decreases to 3.7 eV relative to 4.3 eV at 300 K, indicating a 0.6-eV increase in the intramolecular Coulomb repulsion between the two carboxylates in the folded conformation. A systematic temperature-dependent study was performed on the $n = 14$ hydrated clusters with a temperature gradient of 5 K from 150 K down to 18 K. The ratio of the folded-over linear conformations can be precisely controlled as a function of temperature, yielding the enthalpy and entropy differences between the two conformations. A folding barrier was also observed at very low temperatures, resulting in kinetic trapping of the linear conformation (135).

5.2. Probing the Electronic Structure of Multiply Charged Transition-Metal Complexes

Although many inorganic metal complexes have been studied extensively in the condensed phase for many decades, gas-phase studies of these species are limited and are desirable for obtaining information about their intrinsic molecular properties without the complications of the condensed-phase environments. The ESI-PES apparatus is ideally suitable to study these species in the gas phase and to obtain electronic structure information for such metal complexes as long as they are long-lived in the gas phase. A series of transition-metal halide complexes (101, 103, 105) and biologically relevant molecules such as cubane [4Fe-4S] cluster dianions (112–119) have been studied. This work has stimulated two recent theoretical studies on the PtX_6^{2-} halide complexes (144, 145), revealing the important interplay of electron correlation and relativistic effects.

The low-temperature apparatus is ideally suited to study both singly and multiply charged metal complex anions, owing to the elimination of vibrational hot bands. The low-temperature spectra can yield more detailed electronic structure information, which would otherwise be smeared out at room temperature. A low-temperature PES and theoretical study on $Pt(CN)_n^{2-}$ ($n = 4, 6$) has been reported (132), and a detailed PES study was performed on the electronic structures of transition-metal bis(dithiolene) centers $[M(mnt)_2]^{2-}$ [M = Fe–Zn, Ni, Pd, Pt; mnt = 1,2-$S_2C_2(CN)_2$] (130, 131), which exhibit interesting redox, magnetic, and optical properties in the condensed phase. **Figure 7** shows the 70-K PES spectra of $[M(mnt)_2]^{2-}$ (M = Fe–Zn) at different photon energies (131). Significant changes are observed for the $[M(mnt)_2]^{2-}$ dianions owing to stabilization of the metal 3*d* levels from Fe to Zn and the transition from square-planar to tetrahedral coordination about the metal center, D_{2h} (Fe–Ni) → D_2 (Cu) → D_{2d} (Zn). The combined data illustrate the subtle interplay between metal- and ligand-based redox chemistry in these species and demonstrate changes in their electronic structures with the metal center, oxidation state, and coordination geometry.

5.3. Low-Temperature Photoelectron Spectroscopy of C_{70}^{2-} and Higher Fullerene Dianions

Although C_{60}^{2-} and C_{70}^{2-} are among the first dianions observed in the gas phase by mass spectrometry (54, 55), their gaseous spectroscopic study remained elusive. The stabilities of the fullerene dianions are expected to increase with the fullerene cage size. Indeed higher fullerene dianions, C_n^{2-} ($n = 76, 78, 84$), were readily generated by ESI (69, 70, 123, 124). Their PES spectra were first recorded at relatively low resolution at room temperature (123, 124). The high internal energy distributions inherent in these relatively large molecular dianions resulted in long thermal tails in the PES spectra, which complicated the determination of the ADEs and generally led to

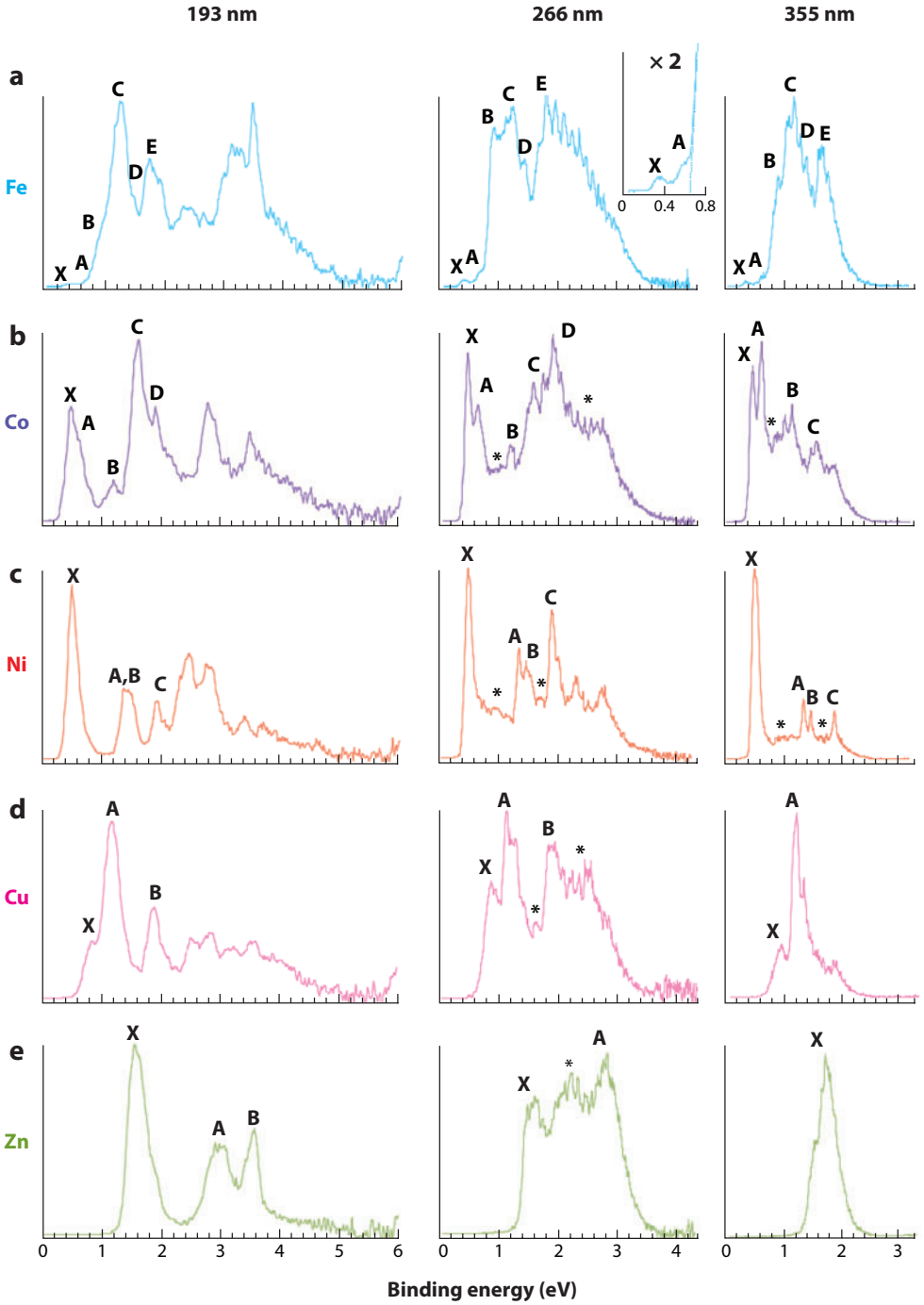

Figure 7

70-K photoelectron spectra measured at 193 nm (*left column*), 266 nm (*middle column*) and 355 nm (*right column*) for (*a*) $[Fe(mnt)_2]^{2-}$, (*b*) $[Co(mnt)_2]^{2-}$, (*c*) $[Ni(mnt)_2]^{2-}$, (*d*) $[Cu(mnt)_2]^{2-}$, and (*e*) $[Zn(mnt)_2]^{2-}$. The inset in the 266-nm spectrum of $[Fe(mnt)_2]^{2-}$ is an expansion of the region 0–0.8 eV to illustrate features X and A more clearly. Features marked with an asterisk in the 266- and 355-nm spectrum were not observed at 193 nm and are assumed to result from autodetachment or multielectron processes. Figure reprinted from Reference 131.

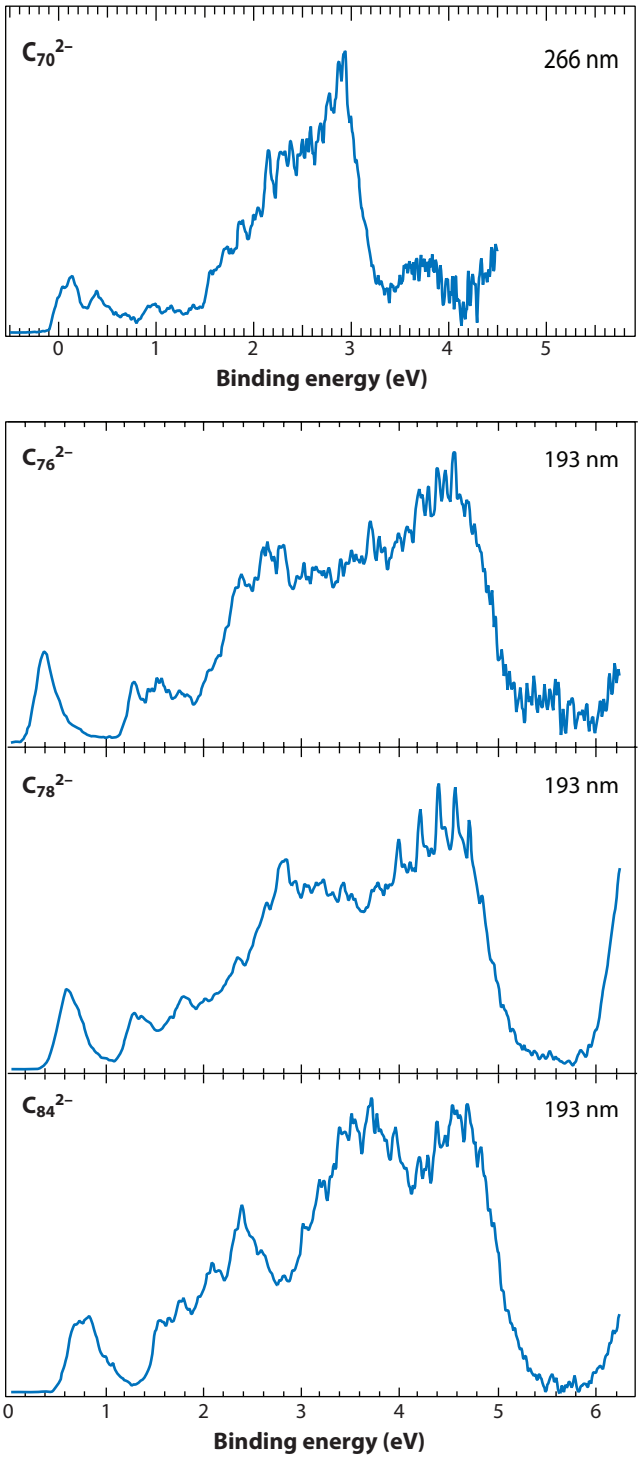

Figure 8

70-K photoelectron spectra of C_{70}^{2-} at 266 nm (4.661 eV) and higher fullerene dianions, C_n^{2-} (n = 76, 78, 84), at 193 nm (6.424 eV). Note the adiabatic detachment energy is near zero for C_{70}^{2-} and increases with cage size.

lower ADE values. For example, the extrapolated ADE of C_{70}^{2-} based on the reported ADEs of C_{76}^{2-}, C_{78}^{2-}, and C_{84}^{2-} was −0.28 eV, which was lower than the true ADE of C_{70}^{2-} by 0.3 eV (see below).

The C_{70}^{2-} dianion was produced, using the low-temperature ESI-PES apparatus, and vibrationally cold PES spectra were obtained for this elusive species (**Figure 8**) (133). The dianion C_{70}^{2-} is the smallest stable fullerene dianion with a positive, albeit small, ADE of 0.02 eV. Cold PES spectra for C_n^{2-} and C_n^{-} (n = 76, 78, 84) were also obtained (**Figure 8**) (134). Significant improvements were observed in the cold spectra, which show well-resolved electronic structures, particularly at the threshold regions, at which sharp 0–0 transitions are resolved for all higher fullerene dianions (127). The ADEs measured from the 0–0 peaks are significantly higher than the previous estimations by ∼0.3 eV. As shown in **Figure 9** for C_{78}^{2-} and C_{84}^{2-}, the cold spectra allow isomer-specific information to be obtained, which is not possible at room temperature.

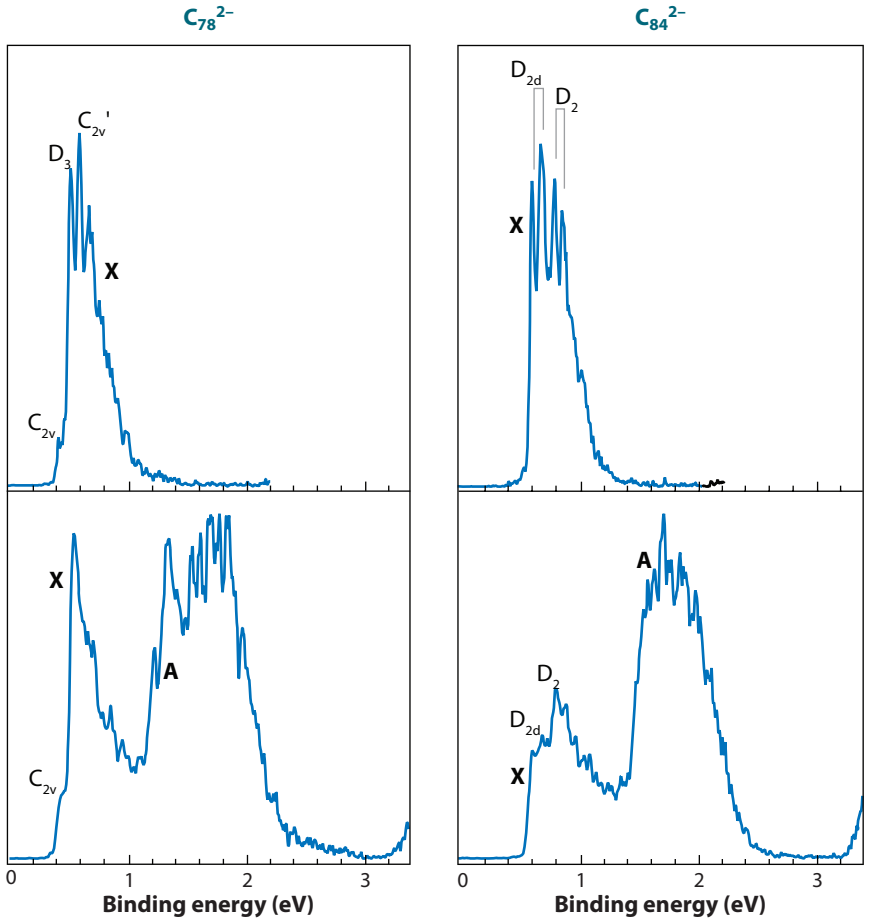

Figure 9

70-K photoelectron spectra of C_{78}^{2-} (*left panels*) and C_{84}^{2-} (*right panels*) at 532-nm (*upper row*) and 355-nm (*lower row*) photon energies. Note that the three isomers of C_{78} (C_{2v}, D_3, and C_{2v}') and two isomers of C_{84} (D_2, D_{2d}) are clearly distinguished owing to the vibrational cooling.

6. PERSPECTIVE AND CONCLUSIONS

This review presents an overview of recent experimental advances on the application of photodetachment PES for free and solvated MCAs. These results demonstrate the power and versatility of the photodetachment technique to probe the properties of free MCAs, and in general solution-phase chemistry and species in the gas phase. Although the research field has rapidly developed during the past decade, much remains to be done. One can expect that with the development of new experimental techniques, many other properties about gaseous MCAs can be studied. One example is the recently developed low-temperature ion trap, which has demonstrated the potential to allow isolated as well as solvated MCAs to be probed under well-defined temperatures by either PES (127–135) or infrared action spectroscopy (146, 147). Dramatic infrared or photoelectron spectral improvements have been achieved for cold anions, yielding detailed electronic and geometric structure information. Furthermore, temperature-dependent studies are now possible, which can be used to investigate entropic effects on ion conformations and isomer populations.

SUMMARY POINTS

1. Photodetachment PES combined with ESI provides a general and sensitive spectroscopic tool to probe the stability and electronic structures of free MCAs, as well as any solution-phase anions in the gas phase. The existence of the RCB was directly observed in PES, and its magnitude can be estimated by photon-dependent PES.
2. The RCB has a profound influence on properties of MCAs and their photoelectron spectra. It provides dynamic stability for MCAs and can even trap unbound electrons. Negative electron binding energies have been observed in several MCAs.
3. The solvation and solvent stabilization of small MCAs such as SO_4^{2-} and $C_2O_4^{2-}$ have been studied, which each require a minimum of three water molecules to be stabilized in the gas phase. Water molecules are found to nucleate around the SO_4^{2-} and $C_2O_4^{2-}$ solutes, giving rise to bulk instead of surface solvation.
4. Solvent-mediated, temperature-dependent folding of $^{-}O_2C\text{-}(CH_2)_6\text{-}CO_2^{-}$ (suberate) has been studied. For small solvated clusters, both $\text{-}CO_2^{-}$ groups are separately solvated in an alternating pattern, giving rise to two isolated solvation centers bridged by the $\text{-}(CH_2)_6\text{-}$ hydrophobic chain in an overall linear conformation. Upon the addition of more water, the suberate dianion folds because the merging of the two water droplets provides additional cooperative hydrogen-bonding interactions that overcome the resulting increase in Coulomb repulsion. The folding transition is observed to occur at 16 water molecules at room temperature and is decreased to 14 water molecules below 120 K owing to the entropic effect. Systematic temperature-dependent studies have yielded quantitative thermodynamic information between the linear and folded conformations.
5. The electronic structures and stability of metal complexes and fullerene dianions, C_n^{2-} (n = 70, 76, 78, 84), have been investigated at low temperatures. Drastic PES spectral improvements have been achieved for the vibrationally cold anions, yielding rich electronic structure and more accurate energetic information.

6. A new low-temperature PES instrument has been developed, showing promise to eliminate thermal broadening and help stabilize weakly bound species. Temperature-dependent studies are made possible for weakly bound molecular and solvated clusters, allowing thermodynamic information to be obtained. It is anticipated that the temperature control capability using a simple Paul trap will significantly expand the potentials to study solution-phase species in the gas phase.

DISCLOSURE STATEMENT

The authors are not aware of any biases that might be perceived as affecting the objectivity of this review.

ACKNOWLEDGMENT

The work described in this article was supported by the U.S. Department of Energy, Office of Basic Energy Sciences, Chemical Science Division, and the National Science Foundation and was performed at the W.R. Wiley Environmental Molecular Sciences Laboratory, a national scientific user facility sponsored by DOE's Office of Biological and Environmental Research and located at Pacific Northwest National Laboratory, which is operated for DOE by Battelle.

LITERATURE CITED

1. Scheller MK, Compton RN, Cederbaum LS. 1995. Gas-phase multiply charged anions. *Science* 270:1160–66
2. Kalcher J, Sax AF. 1994. Gas phase stability of small anions: theory and experiment in cooperation. *Chem. Rev.* 94:2291–318
3. Freeman GR, March NH. 1996. Chemistry of multiply charged negative molecular ions and clusters in the gas phase: terrestrial and in intense galactic magnetic fields. *J. Phys. Chem.* 100:4331–38
4. Boldyrev AI, Simons J. 1994. Isolated SO_4^{2-} and PO_4^{3-} anions do not exist. *J. Phys. Chem.* 98:2298–300
5. Dougherty RC. 1969. Negative-ion mass spectrum of benzol[cd]-pyrene-6-one: evidence for a doubly charged negative ion in the gas phase. *J. Chem. Phys.* 50:1896–97
6. Bowie JH, Stapleton BJ. 1976. Electron impact studies. C. Doubly charged negative ions. *J. Am. Chem. Soc.* 98:6480–83
7. Maas WPM, Nibbering NMM. 1989. Formation of doubly charged negative ions in the gas phase by collisionally-induced "ion pair" formation from singly charged negative ions. *Int. J. Mass Spectrom. Ion Process.* 88:257–66
8. Siu KWM, Gardner GJ, Berman SS. 1989. Multiply charged ions in ionspray tandem mass spectrometry. *Org. Mass Spectrom.* 24:931–42
9. Schauer SN, Williams P, Compton RN. 1990. Production of small doubly charged negative carbon cluster ions by sputtering. *Phys. Rev. Lett.* 65:625–28
10. Miyoshi E, Sakai Y. 1988. Theoretical study on electronic structures of AuF_6 and its anions. *J. Chem. Phys.* 89:7363–66
11. Gutsev GL, Boldyrev AI. 1990. Theoretical estimation of the maximal value of the first, second, and higher electron affinity of chemical compounds. *J. Phys. Chem.* 94:2256–59
12. Ewig CS, Van Wazer JR. 1990. Ab initio studies of molecular structures and energetics. 4. Hexacoordinated NF_6^- and CF_6^{2-} anions. *J. Am. Chem. Soc.* 112:109–14
13. Hotokka M, Pyykkö P. 1989. An ab initio study of bonding trends in the series BO_3^{2-}, CO_3^{2-}, NO_3^- and $O_4(D_{3h})$. *Chem. Phys. Lett.* 157:415–18

14. Weikert HG, Cederbaum LS, Tarantelli F, Boldyrev AI. 1991. On the existence of free doubly negative molecular ions. *Z. Phys. D* 18:299–305
15. Sommerfeld T, Scheller MK, Cederbaum LS. 1993. The structure of small doubly negative carbon clusters. *Chem. Phys. Lett.* 209:216–22
16. Scheller MK, Cederbaum LS. 1993. Stability of MX_3^{2-} ions in the gas phase and when do ionic molecules have large ionization potentials. *J. Chem. Phys.* 99:441–55
17. Scheller MK, Cederbaum LS. 1994. Construction principle for stable multiply-negative charged molecular systems. Part I. Doubly-negative charged systems. *J. Chem. Phys.* 100:8934–42
18. Scheller MK, Cederbaum LS. 1994. Construction principle for stable multiply-negative charged molecular systems. Part II. Triply-negative charged systems. *J. Chem. Phys.* 100:8943–55
19. Sommerfeld T, Scheller MK, Cederbaum LS. 1994. Small dianionic carbon clusters: general aspects on their stability and results for C_9^{2-}. *J. Phys. Chem.* 98:8914–20
20. Sommerfeld T, Scheller MK, Cederbaum LS. 1995. A new class of free stable doubly negative systems: first investigations on the $Si_mO_n^{2-}$ series. *J. Chem. Phys.* 103:1057–63
21. Berghof V, Sommerfeld T, Cederbaum LS. 1998. Sulfur cluster dianions. *J. Phys. Chem. A* 102:5100–5
22. Dreuw A, Sommerfeld T, Cederbaum LS. 1998. Mixed silicon-carbon dianions and their stability in the gas phase. *J. Chem. Phys.* 109:2727–36
23. Sommerfeld T, Child MS. 1999. Dissociation lifetimes of alkali halide dianions. *J. Chem. Phys.* 110:5670–76
24. Dreuw A, Cederbaum LS. 2000. Tunneling lifetimes of metastable and binding properties of stable covalent BeC_n^{2-} ($n = 4, 6$) dianions. *J. Chem. Phys.* 112:7400–8
25. Dreuw A, Cederbaum LS. 2000. Nature of the repulsive Coulomb barrier in multiply charged negative ions. *Phys. Rev. A* 63:012501
26. Dreuw A, Cederbaum LS. 2002. Multiply charged anions in the gas phase. *Chem. Rev.* 102:181–200
27. Dreuw A, Schweinsberg H, Cederbaum LS. 2002. Long-lived gas-phase dianions containing tetrahedrally coordinated oxygen atoms: $O(BN)_4^{2-}$ and $O(C_2)_4^{2-}$. *J. Phys. Chem. A* 106:1406–8
28. Gnaser H, Dreuw A, Cederbaum LS. 2002. Discovery of a new class of stable gas-phase dianions: mixed oxygen-carbon cluster OC_n^{2-} ($n = 5$–19). *J. Chem. Phys.* 117:7002–9
29. Feuerbacher S, Cederbaum LS. 2003. Influence of delocalization on the stability of dianions: study of a systematic series of dianions with growing electronic localization. *J. Am. Chem. Soc.* 125:9531–37
30. Boldyrev AI, Simons J. 1992. Is TeF_8^{2-} the MX_n^{2-} dianion with the largest electron detachment energy (5 eV)? *J. Chem. Phys.* 97:2826–27
31. Boldyrev AI, Simons J. 1993. Theoretical search for small linear doubly charged anions. *J. Chem. Phys.* 98:4745–52
32. Gutowski M, Boldyrev AI, Ortiz JV, Simons J. 1994. Vertical electron detachment energies for octahedral closed-shell multiply-charged anions. *J. Am. Chem. Soc.* 116:9262–68
33. Gutowski M, Boldyrev AI, Simons J, Rak J, Blazejowski J. 1996. Properties of closed-shell, octahedral, multiply-charged hexafluorometallates MF_6^{3-}, M = Sc, Y, La, ZrF_6^{2-}, and TaF_6^-. *J. Am. Chem. Soc.* 118:1173–80
34. Boldyrev AI, Gutowski M, Simons J. 1996. Small multiply charged anions as building blocks in chemistry. *Acc. Chem. Res.* 29:497–502
35. Skurski P, Gutowski M, Simons J. 1999. Mixed valence/dipole-bound dianions. *J. Chem. Phys.* 111:9469–74
36. Skurski P, Simons J. 2000. A dipole-bound dianion. *J. Chem. Phys.* 112:6563–70
37. Adamowicz L. 1991. Theoretical study of doubly charged negative ions of elemental clusters: stability of C_8^{2-}. *J. Chem. Phys.* 95:8669–70
38. Watts JD, Bartlett RJ. 1992. A theoretical study of liner carbon cluster monoanions, C_n^-, and dianions, C_n^{2-} ($n = 2$–10). *J. Chem. Phys.* 97:3445–57
39. Zakrzewski VG, Ortiz JV. 1995. Electron propagator calculations on linear and branched carbon cluster dianions. *J. Chem. Phys.* 102:294–300
40. Dolgounitcheva O, Zakrzewski VG, Ortiz JV. 1998. Structure, bonding, and energetics of C_7^{2-} isomers. *J. Chem. Phys.* 109:87–93

41. McKee ML. 1996. Computational study of the mono- and dianions of SO_2, SO_3, SO_4, S_2O_3, S_2O_4, S_2O_6 and S_2O_8. *J. Phys. Chem.* 100:3473–81
42. Herbert JM, Ortiz JV. 2000. Ab initio investigation of electron detachment in dicarboxylate dianions. *J. Phys. Chem. A* 104:11786–95
43. Enlow M, Ortiz JV. 2002. Aromatic carboxylate superhalogens and multiply charged anions. *J. Phys. Chem. A* 106:5373–79
44. Gutowski M, Rak J, Dokurno P, Blazejowski J. 1994. Theoretical studies on the structures, thermochemistry, vibrational spectroscopy, and other features of HfX_6^{2-} (X = F, Cl, Br, I): electrostatic energy in hexahalogenhafnates. *Inorg. Chem.* 33:6187–93
45. Drake GW, Dixon DA, Sheehy JA, Boatz JA, Christe KO. 1998. Seven-coordinated pnicogens: synthesis and characterization of the SbF_7^{2-} and BiF_7^{2-} dianions and a theoretical study of the AsF_7^{2-} dianion. *J. Am. Chem. Soc.* 120:8392–400
46. Yannouleas C, Landman U. 1993. Multiply charged anionic metal clusters. *Chem. Phys. Lett.* 210:437–42
47. Yannouleas C, Landman U. 1994. Stabilized-jellium description of neutral and multiply charged fullerenes $C_{60}^{x\pm}$. *Chem. Phys. Lett.* 217:175–85
48. Yannouleas C, Landman U. 2000. Decay channels and appearance sizes of doubly anionic gold and silver clusters. *Phys. Rev. B* 61:R10587–89
49. Shi Q, Kais S. 2002. Lifetimes of metastable spherical carbon cluster dianions. *Mol. Phys.* 100:475–81
50. Shi Q, Kais S. 2002. The repulsive Coulomb barrier along a dissociation path of the BeC_4^{2-} dianion. *J. Am. Chem. Soc.* 124:11723–29
51. Gnaser H, Oechsner H. 1993. A search for doubly negative cluster ions in sputtering. *Nucl. Instrum. Methods Phys. Res. B* 82:518–21
52. Middleton R, Klein J. 1997. Carbon anions and dianion clusters. *Nucl. Instrum. Methods Phys. Res. B* 123:532–38
53. Calabrese D, Covington AM, Thompson JS. 1996. Evidence of small odd-numbered dianionic carbon cluster beams from a cesium-sputter negative ion source. *J. Chem. Phys.* 105:2936–37
54. Hettich RL, Compton RN, Ritchie RH. 1991. Doubly charged negative ions of carbon-60. *Phys. Rev. Lett.* 67:1242–45
55. Limbach PA, Schweikhard L, Cowen KA, McDermott MT, Marshall AG, Coe JV. 1991. Observation of the doubly charged, gas-phase fullerene anions C_{60}^{2-} and C_{70}^{2-}. *J. Am. Chem. Soc.* 113:6795–98
56. Jin C, Hettich RL, Compton RN, Tuinman AA, Derecskei-Kovacs A, et al. 1994. Attachment of two electrons to $C_{60}F_{48}$: Coulomb barriers in doubly charged anions. *Phys. Rev. Lett.* 73:2821–24
57. Compton RN, Tuinman AA, Klots CE, Pederson MR, Patton DC. 1997. Electron attachment to a negative ion: $e + C_{84}^{-} = C_{84-}^{2}$. *Phys. Rev. Lett.* 78:4367–70
58. Tuinman AA, Compton RN. 2002. Doubly charged negative ions via charge-exchange collisions: $C_{60}F_{36}^{-} + CH_4 \rightarrow C_{60}F_{36--}^{2} + CH_4^{+}$. *Phys. Rev. A* 65:052724
59. Klein J, Middleton R. 1999. Observation of BeC_n^{2-}, a particularly abundant gaseous dianion. *Nucl. Instrum. Methods Phys. Res. B* 159:8–21
60. Middleton R, Klein J. 1999. Experimental verification of the existence of the gas-phase dianions BeF_4^{2-} and MgF_4^{2-}. *Phys. Rev. A* 60:3515–21
61. Gnaser H. 1999. Doubly charged negative silicon-carbon clusters produced in sputtering. *Phys. Rev. A* 60:R2645–48
62. Berkovits D, Heber O, Klein J, Mitnik D, Paul M. 2000. Photodissociation of the free BeC_6^{2-} dianion. *Nucl. Instrum. Methods Phys. Res. B* 172:350–54
63. Blades AT, Kebarle P. 1994. Study of the stability and hydration of doubly charged ions in the gas phase: SO_4^{2-}, $S_2O_6^{2-}$, $S_2O_8^{2-}$, and some related species. *J. Am. Chem. Soc.* 116:10761–66
64. Blades AT, Klassen JS, Kebarle P. 1995. Free energies of hydration in the gas phase of the anions of some oxo acids of C, N, S, P, Cl, and I. *J. Am. Chem. Soc.* 117:10563–71
65. Blades AT, Ho Y, Kebarle P. 1996. Free energies of hydration in the gas phase of some phosphate singly and doubly charged anions: $(HO)_2PO_2^{-}$ (orthophosphate), $(HO)O_2POPO_2(OH)^{2-}$ (diphosphate), ribose 5-phosphate, adenosine 5′-phosphate, and adenosine 5′-diphosphate. *J. Phys. Chem.* 100:2443–46

66. Arthur TB, Peschke M, Kebarle P. 2003. Hydration of cyclic oxocarbon dianions, such as c-$C_5O_5^{2-}$, in the gas phase: charge reduction of hydrates by electron detachment or proton transfer energy barriers for electron detachment and electron transfer. *Int. J. Mass Spectrom.* 228:1017–34
67. Lau TC, Wang J, Siu KWM, Guevremont R. 1994. Electrospray tandem mass spectrometry of oxo complexes of chromium, manganese and ruthenium. *J. Chem. Soc. Chem. Commun.* 1994:1487–88
68. Lau TC, Wang J, Guevremont R, Siu KWM. 1995. Electrospray tandem mass spectrometry of polyoxoanions. *J. Chem. Soc. Chem. Commun.* 1995:877–78
69. Khairallah G, Peel JB. 1997. Identification of cyano dianions of C_{60} by electrospray mass spectrometry. *Chem. Phys. Lett.* 268:218–22
70. Khairallah G, Peel JB. 1998. Identification of dianions of C_{84} and C_{90} by electrospray mass spectrometry. *Chem. Phys. Lett.* 296:545–48
71. Tuinman AA, Compton RN. 1998. Structures of gas-phase $(C_{60})_n(CN)_m$ trianions from reactions of C_{60} with NaCN in solution. *J. Phys. Chem. A* 102:9791–96
72. Raymond CC, Dick DL, Dorhout PK. 1997. Speciation of main-group metal ions by electrospray mass spectrometry. 1. Investigation of aqueous polyselenide species and effects of cations and pH. *Inorg. Chem.* 36:2678–81
73. Yannouleas C, Landman U, Herlert A, Schweikhard L. 2001. Multiply charged metal cluster anions. *Phys. Rev. Lett.* 86:2996–99
74. Herlert A, Jertz R, Otamendi JA, Martinez AJG, Schweikhard L. 2002. The influence of the trapping potential on the attachment of a second electron to stored metal cluster and fullerene anions. *Int. J. Mass Spectrom.* 218:217–25
75. Lassesson A, Walsh N, Martinez F, Herlert A, Marx G, Schweikhard L. 2005. Formation of fullerene dianions in a Penning trap. *Eur. Phys. J. D* 34:73–77
76. Stoermer C, Friedrich J, Kappes MM. 2001. Observation of multiply charged cluster anions upon pulsed UV laser ablation of metal surfaces under high vacuum. *Int. J. Mass Spectrom.* 206:63–78
77. Zhao XL, Litherland AE. 2005. Observation of LiF_3^{2-}. *Phys. Rev. A* 71:064501
78. Franzreb K, Williams P. 2005. Small gas-phase dianions produced by sputtering and gas flooding. *J. Chem. Phys.* 123:224312
79. Boltalina OV, Hvelplund P, Larsen MC, Larsson MO. 1998. Electron capture by $C_{60}F_{35}^-$ in collisions with atomic and molecular targets. *Phys. Rev. Lett.* 80:5101–4
80. Liu B, Tomita S, Rangama J, Hvelplund P, Nielsen SB. 2003. Electron attachment to "naked" and microsolvated nucleotide anions: detection of long-lived dianions. *Chem. Phys. Chem.* 4:1341–44
81. Liu B, Hvelplund P, Nielsen SB, Tomita S. 2004. Formation of C_{60}^{2-} dianions in collisions between C_{60}^- and Na atoms. *Phys. Rev. Lett.* 92:168301
82. Boltalina OV, Streletskii AV, Loffe IN, Hvelplund P, Liu B, et al. 2005. Formation of long-lived fluorofullerene trianions in collisions with Na. *J. Chem. Phys.* 122:021102
83. Tomita S, Andersen JU, Cederquist H, Concina B, Echt O, et al. 2006. Lifetimes of C_{60}^{2-} and C_{70}^{2-} dianions in a storage ring. *J. Chem. Phys.* 124:024310
84. Bojesen G, Hvelplund P, Jørgensen TJD, Nielsen SB. 2000. Probing the lowest coordination number of dianionic platinum-cyanide complexes in the gas phase: dynamics of the charge dissociation process. *J. Chem. Phys.* 113:6608–12
85. Nielsen AB, Hvelplund P, Liu B, Nielsen SB, Tomita S. 2003. Coulomb explosion upon electron attachment to a four-coordinate monoanionic metal complex. *J. Am. Chem. Soc.* 125:9592–93
86. Boxford WE, El Ghazaly MOA, Dessent CEH, Nielsen SB. 2005. High-energy collision induced dissociation of iridium hexa-halide dianions: observation of triple electron detachment and other decay pathways. *Int. J. Mass Spectrom.* 244:60–64
87. Wong RL, Williams ER. 2003. Dissociation of $SO_4^{2-}(H_2O)_n$ clusters, $n = 3$–17. *J. Phys. Chem. A* 107:10976–83
88. Boxford WE, Pearce JK, Dessent CEH. 2004. Ionic fragmentation versus electron detachment in isolated transition metal complex dianions. *Chem. Phys. Lett.* 399:465–70
89. Burke RM, Pearce JK, Boxford WE, Bruckmann A, Dessent CEH. 2005. Stabilization of excess charge in isolated adenosine 5′-triphosphate and adenosine 5′-diphosphate multiply and singly charged anions. *J. Phys. Chem. A* 109:9775–85

90. Burke RM, Boxford WE, Dessent CEH. 2006. Counter-ion perturbation of the fragmentation pathways of multiply charged anions: evidence for exit channel complexes on the fragmentation potential energy surfaces. *J. Chem. Phys.* 125:021105
91. Boxford WE, Dessent CEH. 2006. Probing the intrinsic features and environmental stabilization of multiply charged anions. *Phys. Chem. Chem. Phys.* 8:5151–65
92. Blom MN, Hampe O, Gilb S, Weis P, Kappes MM. 2001. Tunneling electron loss from isolated platinum tetrahalide dianions. *J. Chem. Phys.* 115:3690–97
93. Yamashita M, Fenn JB. 1984. Electrospary ion source: another variation on the free-jet theme. *J. Phys. Chem.* 88:4451–59
94. Yamashita M, Fenn JB. 1984. Negative ion production with the electrospray ion source. *J. Phys. Chem.* 88:4671–75
95. Wang LS, Ding CF, Wang XB, Barlow SE. 1999. Photodetachment photoelectron spectroscopy of multiply charged anions using electrospray ionization. *Rev. Sci. Instrum.* 70:1957–66
96. Wang XB, Ding CF, Wang LS. 1998. Photodetachment spectroscopy of a doubly charged anion: direct observation of the repulsive Coulomb barrier. *Phys. Rev. Lett.* 81:3351–54
97. Wang LS, Ding CF, Wang XB, Nicholas JB. 1998. Probing the potential barriers and intramolecular electrostatic interactions in free doubly charged anions. *Phys. Rev. Lett.* 81:2667–70
98. Ding CF, Wang XB, Wang LS. 1998. Photoelectron spectroscopy of doubly charged anions: intramolecular Coulomb repulsion and solvent stabilization. *J. Phys. Chem. A* 102:8633–36
99. Ding CF, Wang XB, Wang LS. 1999. Photodetachment photoelectron spectroscopy of doubly charged anions: $S_2O_8^{2-}$. *J. Chem. Phys.* 110:3635–38
100. Wang XB, Ding CF, Wang LS. 1999. Electron tunneling through the repulsive Coulomb barrier in photodetachment of multiply charged anions. *Chem. Phys. Lett.* 307:391–96
101. Wang XB, Wang LS. 1999. Photodetachment of free hexahalogenometallate doubly charged anions in the gas phase: $[ML_6]^{2-}$ (M = Re, Os, Ir, Pt; L = Cl and Br). *J. Chem. Phys.* 111:4497–509
102. Wang XB, Wang LS. 1999. Observation of negative electron-binding energy in a molecule. *Nature* 400:245–48
103. Wang XB, Wang LS. 1999. Experimental search for the smallest stable multiply-charged anions in the gas phase. *Phys. Rev. Lett.* 83:3402–5
104. Wang LS, Wang XB. 2000. Probing free multiply charged anions using photodetachment photoelectron spectroscopy. *J. Phys. Chem. A* 104:1978–90
105. Wang XB, Wang LS. 2000. Probing the electronic structure and metal-metal bond of $Re_2Cl_8^{2-}$ in the gas phase. *J. Am. Chem. Soc.* 122:2096–100
106. Wang XB, Nicholas JB, Wang LS. 2000. Electronic instability of isolated SO_4^{2-} and its solvation stabilization. *J. Chem. Phys.* 113:10837–40
107. Wang XB, Yang X, Nicholas JB, Wang LS. 2001. Bulk-like features in the photoemission spectra of hydrated doubly-charged anion clusters. *Science* 294:1322–25
108. Wang XB, Yang X, Nicholas JB, Wang LS. 2003. Photodetachment of hydrated oxalate dianions in the gas phase, $C_2O_4^{2-}(H_2O)_n$ (n = 3–40): from solvated clusters to nanodroplet. *J. Chem. Phys.* 119:3631–40
109. Wang XB, Yang X, Wang LS. 2002. Probing solution phase species and chemistry in the gas phase. *Int. Rev. Phys. Chem.* 21:473–98
110. Yang X, Fu YJ, Wang XB, Slavicek P, Mucha M, et al. 2004. Solvent-mediated folding of a doubly charged anion. *J. Am. Chem. Soc.* 126:876–83
111. Minofar B, Mucha M, Jungwirth P, Yang X, Fu YJ, et al. 2004. Bulk versus interfacial aqueous solvation of dicarboxylate dianions. *J. Am. Chem. Soc.* 126:11691–98
112. Wang XB, Inscore FE, Yang X, Cooney JJA, Enemark JH, Wang LS. 2002. Probing the electronic structure of $[MoOS_4]^-$ centers using anionic photoelectron spectroscopy. *J. Am. Chem. Soc.* 124:10182–91
113. Yang X, Wang XB, Niu S, Pickett CJ, Ichiye T, Wang LS. 2002. Coulomb- and antiferromagnetic-induced fission in doubly charged cubelike Fe-S clusters. *Phys. Rev. Lett.* 89:163401
114. Wang XB, Niu S, Yang X, Ibrahim SK, Pickett CJ, et al. 2003. Probing the intrinsic electronic structure of the cubane [4Fe-4S] cluster: nature's favorite cluster for electron transfer and storage. *J. Am. Chem. Soc.* 125:14072–81

95. Detailed description of the principle and construction of the first electrospray PES apparatus for MCAs.

96. First PES study of a free MCA and direct observation of the RCB.

97. Determined the relationship between the intramolecular Coulomb repulsion and the RCB in MCAs.

100. Demonstrated the validity of using the tunneling formulism in a-decay for understanding electron tunneling in MCAs.

102. First observation of negative electron binding energy in an MCA.

107. Study on the solvation and solvent stabilization of two unstable textbook dianions, SO_4^{2-} and $C_2O_4^{2-}$, and observation of bulk behavior in solvated clusters, $SO_4^{2-}(H_2O)_n$ and $C_2O_4^{2-}(H_2O)_n$.

115. Yang X, Wang XB, Fu YJ, Wang LS. 2003. On the electronic structure of [1Fe] Fe-S complexes from anionic photoelectron spectroscopy. *J. Phys. Chem. A* 107:1703–9
116. Yang X, Razavet M, Wang XB, Pickett CJ, Wang LS. 2003. Probing the electronic structure of the di-iron subsite of [Fe]-hydrogenase: a photoelectron spectroscopic study of Fe(I)-Fe(I) model complexes. *J. Phys. Chem. A* 107:4612–18
117. Waters T, Wang XB, Yang X, Zhang L, O'Hair RAJ, et al. 2004. Photoelectron spectroscopy of the doubly-charged anions $[M^{IV}O(mnt)_2]^{2-}$ (M = Mo, W; mnt = $S_2C_2(CN)_2{}^{2-}$): access to the ground and excited states of the $[M^{V}O(mnt)_2]^{-}$ anion. *J. Am. Chem. Soc.* 126:5119–29
118. Fu YJ, Yang X, Wang XB, Wang LS. 2005. Probing the electronic structure of [2Fe-2S] clusters with three coordinate iron sites by use of photoelectron spectroscopy. *J. Phys. Chem. A* 109:1815–20
119. Yang X, Wang XB, Fu YJ, Wang LS. 2006. Probing the electronic structure of Fe-S clusters: ubiquitous electron transfer centers in metalloproteins using anion photoelectron spectroscopy in the gas phase. In *Principles of Mass Spectrometry Applied to Biomolecules*, ed. J Laskin, C Lifshitz, 2:63–117. Hoboken: Wiley & Sons
120. Waters T, Wang XB, Wang LS. 2007. Electrospray ionization photoelectron spectroscopy: probing the electronic structure of inorganic metal complexes in the gas phase. *Coord. Chem. Rev.* 251:474–91
121. Friedrich J, Gilb S, Ehrler OT, Behrendt A, Kappes MM. 2002. Electronic photodissociation spectroscopy of isolated $IrX_6{}^{2-}$ (X = Cl, Br). *J. Chem. Phys.* 117:2635–44
122. Löffler D, Weber JM, Kappes MM. 2005. Photodetachment spectroscopy of $PtBr_4{}^{2-}$: probing the Coulomb barrier of a doubly charged anion. *J. Chem. Phys.* 123:224308
123. Ehrler OT, Weber JM, Furche F, Kappes MM. 2003. Photoelectron spectroscopy of C_{84} dianions. *Phys. Rev. Lett.* 91:113006
124. Ehrler OT, Furche F, Weber JM, Kappes MM. 2005. Photoelectron spectroscopy of fullerene dianions $C_{76}{}^{2-}$, $C_{78}{}^{2-}$ and $C_{84}{}^{2-}$. *J. Chem. Phys.* 122:094321
125. Arnold K, Balaban TS, Blom MN, Ehrler OT, Gilb S, et al. 2003. Electron autodetachment from isolated nickel and copper phthalocyanine-tetrasulfonate tetraanions: isomer specific rates. *J. Phys. Chem. A* 107:794–803
126. Ehrler OT, Yang JP, Sugiharto AB, Unterreiner AN, Kappes MM. 2007. Excited state dynamics of metastable phthalocyanine-tetrasulfonate tetra-anions probed by pump/probe photoelectron spectroscopy. *J. Chem. Phys.* 127:184301
127. Wang XB, Woo HK, Wang LS. 2005. Vibrational cooling in a cold ion trap: vibrationally resolved photoelectron spectroscopy of cold $C_{60}{}^{-}$ anions. *J. Chem. Phys.* 123:051106
128. Wang XB, Woo HK, Kiran B, Wang LS. 2005. Observation of weak C-H. . .O hydrogen bonding by unactivated alkanes. *Angew. Chem. Int. Ed. Engl.* 44:4968–72
129. Wang XB, Wang LS. 2008. Development of a low-temperature photoelectron spectroscopy instrument using an electrospray ion source and a cryogenically controlled ion trap. *Rev. Sci. Instrum.* 79:073108
130. Waters T, Woo HK, Wang XB, Wang LS. 2006. Probing the intrinsic electronic structure of the bis(dithiolene) anions $[M(mnt)_2]^{2-}$ and $[M(mnt)_2]^{1-}$ (M = Ni, Pd, Pt; mnt = 1,2-$S_2C_2(CN)_2$) in the gas phase by photoelectron spectroscopy. *J. Am. Chem. Soc.* 128:4282–91
131. Waters T, Wang XB, Woo HK, Wang LS. 2006. Photoelectron spectroscopy of the bis(dithiolene) anions $[M(mnt)_2]^{n-}$ (M = Fe–Zn; n = 1, 2): changes in electronic structure with variation of metal center and with oxidation. *Inorg. Chem.* 45:5841–51
132. Wang XB, Wang YL, Woo HK, Li J, Wu GS, Wang LS. 2006. Free tetra- and hexa-coordinated platinum-cyanide dianions, $Pt(CN)_4{}^{2-}$ and $Pt(CN)_6{}^{2-}$: a combined photodetachment photoelectron spectroscopic and theoretical study. *Chem. Phys.* 329:230–38
133. Wang XB, Woo HK, Huang X, Kappes MM, Wang LS. 2006. Direct experimental probe of the onsite Coulomb repulsion in the doubly charged fullerene anion $C_{70}{}^{2-}$. *Phys. Rev. Lett.* 96:143002
134. Wang XB, Woo HK, Yang J, Kappes MM, Wang LS. 2007. Photoelectron spectroscopy of singly and doubly charged higher fullerenes at low temperatures: $C_{76}{}^{-}$, $C_{78}{}^{-}$, $C_{84}{}^{-}$ and $C_{76}{}^{2-}$, $C_{78}{}^{2-}$, $C_{84}{}^{2-}$. *J. Phys. Chem. C* 111:17684–89
135. Wang XB, Yang J, Wang LS. 2008. Observation of entropic effect on conformation changes of complex systems under well-controlled temperature conditions. *J. Phys. Chem. A* 112:172–75

126. A pump-probe study of electron tunneling dynamics in MCAs.

133. Low-temperature PES study of $C_{70}{}^{2-}$ and direct observation of the onsite Coulomb repulsion.

135. Observation of a temperature-dependent folding transition in a hydrated dicarboxylate dianion.

136. Gilles MK, Polak ML, Lineberger WC. 1992. Photoelectron spectroscopy of the halogen oxide and anions FO^-, ClO^-, BrO^-, IO^-, $OClO^-$, and OIO^-. *J. Chem. Phys.* 96:8012–20
137. Gronert S. 1999. Coulomb repulsion in multiply charged ions: a computational study of the effective dielectric constants of organic spacer groups. *Int. J. Mass Spectrom.* 185:351–57
138. Yang J, Xing XP, Wang XB, Wang LS, Sergeeva AP, Boldyrev AI. 2008. Negative electron binding energies observed in a triply charged anion: photoelectron spectroscopy of 1-hydroxy-3,6,8-pyrene-trisulfonate. *J. Chem. Phys.* 128:091102
139. Stefanovich EV, Boldyrev AI, Truong TN, Simons J. 1998. Ab initio study of the stabilization of multiply charged anions in water. *J. Phys. Chem. B* 102:4205–8
140. Gao B, Liu ZF. 2004. A first principle study on the solvation and structure of $SO_4^{2-}(H_2O)_n$, $n = 6$–12. *J. Chem. Phys.* 121:8299–306
141. Gao B, Liu ZF. 2005. Size-dependent charge-separation reaction for hydrated sulfate dianion cluster, $SO_4^{2-}(H_2O)_n$, with $n = 3$–7. *J. Chem. Phys.* 123:224302
142. Miller Y, Chaban GM, Zhou J, Asmis KR, Neumark DM, Gerber RB. 2007. Vibrational spectroscopy of $(SO_4^{2-})(H_2O)_n$ clusters, $n = 1$–5: harmonic and anharmonic calculations and experiment. *J. Chem. Phys.* 127:094305
143. Jungwirth P, Curtis JE, Tobias DJ. 2003. Polarizability and aqueous solvation of the sulfate dianion. *Chem. Phys. Lett.* 367:704–10
144. Sommerfeld T, Feuerbacher S, Pernpointner M, Cederbaum LS. 2003. Electronic structure of isolated PtX_6^{2-} (X = F, Cl, Br) dianions. *J. Chem. Phys.* 118:1747–55
145. Pernpointner M, Breidbach J, Cederbaum LS. 2005. Remarkable interplay of electron correlation and relativity in the photodetachment spectrum of $PtCl_6^{2-}$. *J. Chem. Phys.* 122:064311
146. Zhou J, Santambrogio G, Brümmer M, Moore DT, Wöste L, et al. 2006. Infrared spectroscopy of hydrated sulfate dianions. *J. Chem. Phys.* 125:111102
147. Bush MF, Saykally RJ, Williams ER. 2007. Evidence for water rings in the hexahydrated sulfate dianion from IR spectroscopy. *J. Am. Chem. Soc.* 129:2220–21

146. Infrared spectroscopic study of cold $SO_4^{2-}(H_2O)_n$ clusters.